Available online at www.sciencedirect.com

SciVerse ScienceDirect

Ceramics International 39 (2013) S331–S334

CERAMICS INTERNATIONAL

www.elsevier.com/locate/ceramint

Microstructure and dielectric properties of $Zn_3Nb_2O_8$ ceramics prepared by a two-stage sintering method

Penphitcha Amonpattaratkit, Athipong Ngamjarurojana, Supon Ananta*

Department of Physics and Materials Science, Faculty of Science, Chiang Mai University, Chiang Mai 50200, Thailand

Available online 26 October 2012

Abstract

In this work, the effects of various two-stage sintering schemes on phase formation, microstructural development and dielectric properties of $Zn_3Nb_2O_8$ ceramics were systematically determined via a combination of scanning electron microscopy (SEM), energy-dispersive X-ray (EDX) and dielectric measurement techniques. In comparison with the conventional sintered samples, it was found that single-phase $Zn_3Nb_2O_8$ ceramics with maximum density of ~99% theoretical density, smaller average grain size (~3 μm) and better dielectric properties can be achieved via a two-stage sintering technique.

Keywords: A. Milling; A. Sintering; B. Grain size; C. Dielectric properties

1. Introduction

Dielectric ceramic resonators have now become the key element in microwave communication systems due to the rapid progress of mobile and satellite communication systems. In connection with this, one of the zinc niobate compounds $Zn_3Nb_2O_8$ ceramic which exhibits good microwave dielectric properties may be developed and applied as dielectric resonators in microwave communication systems. According to the literature, $Zn_3Nb_2O_8$ has high quality factor (> 80,000 GHz [1]), high dielectric constant (~14–22 [2]) and small temperature coefficient of resonance frequency (~ −71 ppm $^{\circ}C^{-1}$ [2–4]). However, the dielectric properties of this material and other microwave dielectric ceramics depend strongly on their microstructures as well as chemical compositions. It was reported earlier that low value of dielectric loss tangent (tan δ) can be revealed if microwave dielectric ceramics of higher density and smaller grain size are achieved [2–4]. Thus, higher density and smaller grain size are essential to achieve optimum dielectric properties. So far, a few studies have reported on the preparation and characterization of $Zn_3Nb_2O_8$ ceramics. For example, Pakawanit and Ananta [5] demonstrated that single-phase $Zn_3Nb_2O_8$ ceramics with maximum density of 98% theoretical density, average grain size ~50 μm and ε_r~22–23 can be obtained by sintering $Zn_3Nb_2O_8$ nanopowders derived from a rapid vibro-milling technique at 1200 °C for 4 h. Moreover, in recent years, Amonpattaratkit et al. [6] also reported the successful preparation of pure phase $Zn_3Nb_2O_8$ ceramics with similar density value but with smaller average grain size (~1 μm) by employing an alternative two-stage sintering technique.

However, interestingly, there is no systematic study on the effect of two-stage sintering technique on microstructure and dielectric properties of $Zn_3Nb_2O_8$ ceramics. Therefore, in this work, the influences of sintering conditions on phase formation, microstructural development and dielectric properties of $Zn_3Nb_2O_8$ ceramics derived from a two-stage sintering technique have been examined and discussed, in comparison with the conventional samples.

2. Experimental procedures

Zinc niobate powders with chemical composition of $Zn_3Nb_2O_8$ were synthesized by the solid state reaction of appropriate amounts of commercially available zinc oxide, ZnO and niobium oxide, Nb_2O_5 (Aldrich, 99.9% purity), as described in detail in our previous works [5–8]. The mixing

*Corresponding author.
E-mail address: suponananta@yahoo.com (S. Ananta).

0272-8842/$ - see front matter © 2012 Elsevier Ltd and Techna Group S.r.l. All rights reserved.
http://dx.doi.org/10.1016/j.ceramint.2012.10.088

Table 1
Physical and dielectric properties of $Zn_3Nb_2O_8$ ceramics sintered at various conditions.

T_1 (°C)	T_2 (°C)	Relative density[a] (%)	Grain size range/mean[b] (μm)	Dielectric properties		
				ε_r	tan δ	
1150	–	96	0.5–7.7/4.1	10.8	0.006	
1150	1050	97	0.4–7.0/3.7	13.0	0.006	
1150	1100	97	0.4–7.2/3.8	16.8	0.004	
1200	–	98	0.3–9.9/5.2	16.3	0.004	
1200	1050	98	0.3–8.2/4.1	14.5	0.006	
1200	1100	99	0.3–6.5/3.4	18.5	0.002	
1200	–	98	20.5–110/50	22.5	–	Ref. [5]
1150	–	93	0.89	–	–	Ref. [3]

[a]Estimated precision of the density is ±1%.
[b]Estimated precision of the grain size is ±0.1%.

process was carried out by vibro-milling (MaCrone Micronizing Mill) a mixture of raw materials for 20 h [5,6] with corundum medium in isopropyl alcohol. After drying at 120 °C for 1 h, the mixtures were calcined in a closed alumina crucible at 1000 °C for 2 h and heating/cooling rates of 10 °C/min [5,6]. Ceramic fabrication was achieved without adding any binders by pressing as pellets (10 mm in diameter and 1.0–1.2 mm thick) in a uniaxial die press at 100 MPa. Green pellets were placed inside a closed alumina crucible and sintered in air at various firing schemes with constant soaking time for 4 h and heating/cooling rates of 5 °C/min. Two sets of the first sintering temperature (T_1) were designed for the two-stage sintering case: 1150 and 1200 °C. Variation of the second sintering temperature (T_2) between 1050 and 1100 °C was carried out for each case (Table 1). Densities of the final sintering ceramics were determined by using the Archimedes principle. Sintered ceramics were examined at room temperature by X-ray diffraction (XRD; Rigako MiniFlex II diffractometer) using Cu Kα radiation to identify the phase formed. The microstructural evolution was characterized using a scanning electron microscope (SEM; JEOL JSM-840A), equipped with an energy-dispersive X-ray (EDX) analyzer. Grain sizes of the sintered ceramics were directly determined from the SEM micrographs.

Before studying the dielectric properties, the samples were lapped to obtain parallel faces. After coating with silver paint as electrode on the face, the samples were heated at 600 °C for 1 h to ensure contact between the electrode and the surface of the ceramic. The dielectric properties were measured by a Precision LCR meter (TH 2819A) at room temperature and a frequency of 100 kHz.

3. Results and discussion

X-ray diffraction patterns of the zinc niobate ceramics two-stage sintered at various conditions (Fig. 1) indicate the formation of only $Zn_3Nb_2O_8$ phase in all cases. The strongest reflections in the majority of all XRD patterns indicate the formation of single-phase $Zn_3Nb_2O_8$ which could be matched with JCPDF no. 79-1164 [9], in agreement with our previous work [6]. There was no evidence of

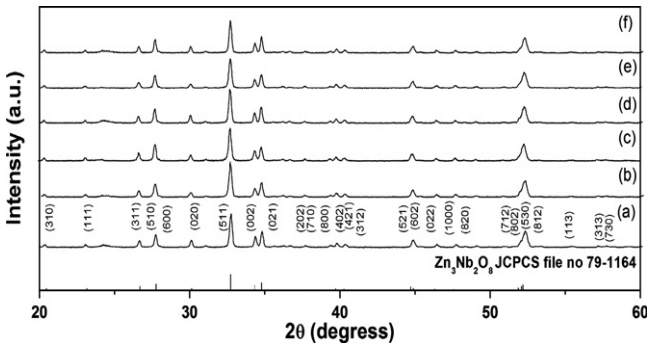

Fig. 1. XRD patterns of the $Zn_3Nb_2O_8$ ceramics sintered at (a) 1150 °C, (b) 1150/1050 °C, (c) 1150/1100 °C, (d) 1200 °C, (e) 1200/1050 °C and (f) 1200/1100 °C for 4 h and heating/cooling rates of 5 °C/min.

unreacted precursors, nor was there any evidence of other secondary phases being present. This observation implies that the two-stage sintering method is an effective process for the production of single-phase $Zn_3Nb_2O_8$ ceramics.

The effects of two-stage sintering conditions on densification and grain size for $Zn_3Nb_2O_8$ ceramics are listed in Table 1. Generally, it is evident that as the sintering temperature increases, the density of almost all the samples increases. Two-stage sintered $Zn_3Nb_2O_8$ ceramics reach a maximum density of ~99% at 1200/1100 °C, each for 4 h (conventional sintered $Zn_3Nb_2O_8$ samples exhibit maximum density of ~98% after sintered at 1200 °C for 4 h [5]).

Moreover, it can be seen that the relative density of the two-stage sintered $Zn_3Nb_2O_8$ ceramics increases from 97% to 99% with increasing sintering temperature, whilst grain size changes only slightly (about 3.7–3.4 μm). This is probably because the two-stage sintering proceeds in a "frozen" microstructure and has effect on grain growth. Hence, the kinetics is sufficient for reaching fairly high density, whilst providing the benefit of suppressing grain growth [10].

Microstructural investigation of the $Zn_3Nb_2O_8$ ceramics sintered at different schemes is shown in Fig. 2. In general, heterogeneous microstructures consisting mainly of two ranges of grains (in respect of size and shape) were found in all samples. The occurrence of a typical abnormal grain growth commonly found in the $Zn_3Nb_2O_8$ ceramics (consistent with

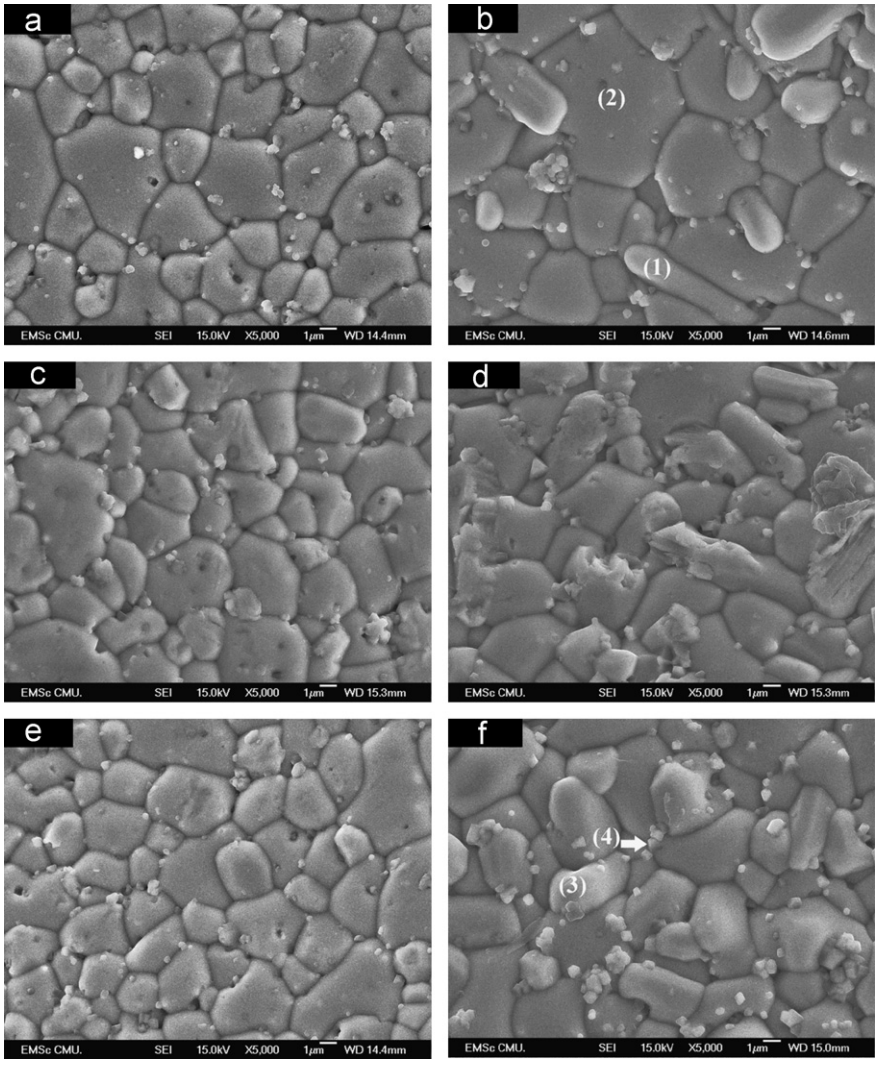

Fig. 2. SEM micrographs of the $Zn_3Nb_2O_8$ ceramics sintered at (a) 1150 °C, (b) 1150/1050 °C, (c) 1150/1100 °C, (d) 1200 °C, (e) 1200/1050 °C and (f) 1200/1100 °C for 4 h and heating/cooling rates of 5 °C/min.

Liou et al. [2], Wu et al. [3] and Pakawanit and Ananta [5]) is also observed after sintering above 1150 °C which could be attributed to atom attachment to surface or boundary steps produced by either two-dimensional nucleation and lateral growth mechanism or the coalescence of grains and the consequent formation of grain boundaries with re-entrant edges [11,12]. For the two-stage sintered samples, it is seen that the average grain size of these ceramics tends to decrease with increasing second firing temperature, in agreement with our previous observation [6]. As given in Table 1, grain size of conventional sintered $Zn_3Nb_2O_8$ ceramics varies greatly from 0.3 to 10 μm whereas the two-stage sintered ceramics contain smaller grain size (~0.3–6.5 μm). By comparison with conventional sintered ceramics (Fig. 2(a) and (d)), denser grain-packing, less abnormal grain growth and small grain size are generally observed in all two-stage sintered samples. This is probably because the two-stage sintering process could suppress the grain growth mechanism. This can explain by the feasibility of densification without grain growth, which is believed to occur in two-stage sintered ceramic, which relies on the suppression of grain boundary migration while keeping grain boundary diffusion active. The kinetic and the driving forces for grain growth behavior in the second-step sintering were previously discussed by Chen and Wang [13]. Their work suggested that the suppression of the final stage grain growth was achieved by exploiting the difference in kinetics between grain-boundary diffusion and grain-boundary migration. By employing a combination of SEM and EDX techniques, more information is obtained as given in Table 2. EDX analysis of the elongated grain (marked as "(1) and (3)") indicated the chemical composition of Nb_2O_5 and ZnO, although the concentration is not found for XRD detection. It is, therefore, intriguing to note the advantage of a combination between SEM and EDX techniques, which lies in their ability to reveal microstructural features of the samples often missed by the XRD diffraction method which requires at least 5 wt% of the component [14]. On the other hand, EDX analyses of the large grain (equiaxed grain; marked as (2)) and small grain (bright area; marked as (4)) indicate the chemical composition neighboring the parent $Zn_3Nb_2O_8$ phase. So,

Table 2
Chemical compositions of $Zn_3Nb_2O_8$ ceramics from EDX analyzer.

EDX positions	Composition (at%)		Possible phases
	Zn (L)	Nb (L)	
(1)	3.91	8.73	Nb_2O_5, ZnO
(2)	11.24	6.85	$Zn_3Nb_2O_8$
(3)	3.95	9.56	Nb_2O_5, ZnO
(4)	7.74	6.02	$Zn_3Nb_2O_8$

increasing the second firing temperature can decrease chemical heterogeneity because different grain shapes of these ceramics tend to decrease with increasing second firing temperature.

These factors are also responsible for the dielectric behavior of the $Zn_3Nb_2O_8$ ceramics. Table 1 also shows the dielectric constant and dielectric loss tangent at 100 kHz at various temperatures. In this case, the $Zn_3Nb_2O_8$ ceramics were sintered via conventional sintering technique. It is seen that the dielectric constant increases with increasing sintering temperature and grain size, which could be attributed to the increasing grain size resulting in reduction of the volume fraction of grain boundaries (i.e. the sink of defects) [4,5], in good agreement with the reports by Wu et al. [3]. Clearly, the increasing dielectric constant is due to the increasing density of these ceramics, in agreement with that in Wongmaneerung et al. [10]. The maximum value of the dielectric constant has been observed in two-stage sintering (1200/1100 °C) which is significantly larger than those observed in the conventional sintered $Zn_3Nb_2O_8$ ceramics. In general, these $Zn_3Nb_2O_8$ ceramics exhibit complex microstructure which is a result of variation in grain morphologies (i.e. size, shape and orientation), densification and the presence of additional minor phase. These factors, which are influenced by the two-stage sintering temperature, have an important effect on the dielectric response of materials and their reproducibility. Here, one can clearly see that the dielectric loss tangent (tan δ) values in two-stage sintered $Zn_3Nb_2O_8$ ceramics are very close to those observed in the conventional sintered $Zn_3Nb_2O_8$. It should be noted that these ceramics have different grain sizes, but similar density values. As expected, samples with the highest density value exhibit the lowest dielectric loss.

4. Conclusions

The influence of two-stage sintering technique on phase formation, microstructural development and dielectric properties of $Zn_3Nb_2O_8$ ceramics was examined. In comparison with the conventional sintered samples, this work demonstrated that pure phase of $Zn_3Nb_2O_8$ ceramics with higher density (~99%), smaller average grain size (~3 μm) and better dielectric properties can be achieved via a two-stage sintering technique.

Acknowledgments

Supports from Synchrotron Light Research Institute (Public Organization), Graduate School and Faculty of Science, Chiang Mai University, are gratefully acknowledged.

References

[1] D.W. Kim, J.H. Kim, J.R. Kim, K.S. Hong, Phase constitutions and microwave dielectric properties of $Zn_3Nb_2O_8$–TiO_2, Japanese Journal of Applied Physics 40 (2001) 5994–5998.
[2] Y.C. Liou, H.M. Chen, W.C. Tsai, Synthesis of $Zn_3Nb_2O_8$ ceramics using a simple and effective process, Ceramics International 35 (2009) 2135–2138.
[3] M.C. Wu, K.T. Huang, W.F. Su, Microwave dielectric properties of doped $Zn_3Nb_2O_8$ ceramics sintered below 950 °C and their compatibility with silver electrode, Materials Chemistry and Physics 98 (2006) 406–409.
[4] A.J. Moulson, J.M. Herbert, Electroceramics, second ed., Wiley, Chichester, 2003.
[5] P. Pakawanit, S. Ananta, Influence of sintering temperature on densification and microstructure of $Zn_3Nb_2O_8$ ceramics derived from nanopowders, Advances in Materials Research 194–196 (2011) 656–659.
[6] P. Amonpattaratkit, P. Pakawanit, S. Ananta, Potential of two-stage sintering technique for fabrication of microwave dielectric $Zn_3Nb_2O_8$ ceramics, in: Proceedings of the 4th International Data Storage Technology Conference of Thailand, 2011, p. 186 [DSTA16].
[7] A. Prasatkhetragarn, R. Yimnirun, S. Ananta, Effect of calcinations conditions on phase formation and particle size of $Zn_3Nb_2O_8$ powders systhesized by solid-state reaction, Materials Letters 61 (2007) 3873–3877.
[8] A. Prasatkhetragarn, P. Ketsuwan, S. Ananta, R. Yimnirun, Effect of vibro-milling time on phase formation and particle size of $Zn_3Nb_2O_8$ nanopowders, Materials Letters 64 (2010) 1113–1116.
[9] Powder Diffraction File no. 79-1164, International Centre for Diffraction Data, Newton Square, PA, 2000.
[10] R. Wongmaneerung, R. Yimnirun, S. Ananta, Effect of two-stage sintering on phase formation, microstructure and dielectric properties of perovskite PMN ceramics derived from a corundum $Mg_4Nb_2O_9$ precursor, Materials Chemistry and Physics 114 (2009) 569–575.
[11] S.B. Lee, N.M. Hwang, D.Y. Yoon, M.F. Henry, Grain boundary faceting and abnormal grain growth in nickel, Metallurgical and Materials Transactions A 31 (2000) 985–994.
[12] H.Y. Lee, J.S. Kim, N.M. Hwang, D.Y. Kim, Effect of sintering temperature on the secondary abnormal grain growth of $BaTiO_3$, Journal of the European Ceramic Society 20 (2000) 731–737.
[13] I.W. Chen, X.H. Wang, Sintering dense nanocrystalline ceramics without final-stage grain growth, Nature 404 (2000) 168–171.
[14] H. Klug, L. Alexander, X-ray Diffraction Procedures For Polycrystalline And Amorphous Materials, second ed., John Wiley & Sons Ltd., New York, 1974.